Nonlinear transport theory for negative-differential resistance states of two-dimensional electron systems in strong magnetic fields

A. Kunold[1,2,*] and M. Torres[3,†]

[1]*INSA-CNRS-UPS, LPCNO, Université de Toulouse, 135 Av. de Rangueil, 31077 Toulouse, France*

[2]*Departamento de Ciencias Básicas, Universidad Autónoma Metropolitana-Azcapotzalco, Avenida San Pablo 180, México, Distrito Federal 02200, México*

[3]*Instituto de Física, Universidad Nacional Autónoma de México, Apartado Postal 20-364, México, Distrito Federal 01000, México*

(Received 3 July 2009; revised manuscript received 16 October 2009; published 13 November 2009)

We present a model to describe the nonlinear response to a direct dc current applied to a two-dimensional electron system in a strong magnetic field. The model is based on the solution of the von Neumann equation incorporating the exact dynamics of two-dimensional damped electrons in the presence of arbitrarily strong magnetic and dc electric fields while the effects of randomly distributed impurities are perturbatively added. From the analysis of the differential resistivity and the longitudinal voltage, we observe the formation of negative-differential resistivity states that are the precursors of the zero-differential resistivity states. Both the effects of elastic impurity scattering as well as those related to inelastic processes play an important role. The theoretical predictions correctly reproduce the main experimental features provided that the inelastic-scattering rate obeys a T^2 temperature dependence, consistent with electron-electron interaction effects.

DOI: 10.1103/PhysRevB.80.205314 PACS number(s): 73.43.Qt, 71.70.Di, 73.43.Cd, 73.50.Bk

I. INTRODUCTION

In the past few years the study of nonlinear transport properties in high mobility two-dimensional electron systems (2DES) has received much attention due to the experimental finding of intense oscillations of the magnetoresistivity and zero resistance states (ZRS). Microwave-induced resistance oscillations (MIRO) were discovered[1–4] in 2DES samples subjected to microwave irradiation and moderate magnetic fields. For the MIRO the photoresistance is a function of the ratio $\epsilon^{\mathrm{ac}}=\omega/\omega_c$, where ω and ω_c are the microwave and cyclotron frequencies, respectively. This outstanding discovery triggered a great amount of theoretical work.[5–17] Our current understanding of this phenomenon rests upon models that predict the existence of negative-resistance states (NRS) yielding an instability that rapidly drives the system into a ZRS.[18] Two distinct mechanisms for the generation of NRS are known, one is based in the microwave-induced impurity scattering[5,7,9–13] while the second is linked to inelastic processes leading to a nontrivial electron distribution function.[8,14,15,17]

An analogous effect, Hall field-induced resistance oscillations (HIRO) has been observed in high mobility samples in response to a dc excitation.[19–22] Although MIRO and HIRO are basically different phenomena both rely on the commensurability of the cyclotron frequency with a characteristic parameter; in both cases oscillations are periodic in $1/B$. In HIRO the oscillation peaks, observed in differential resistance, appear at integer values of the dimensionless parameter $\epsilon^{\mathrm{dc}}=\omega_H/\omega$. Here, $\hbar\omega_H\approx eE_H(2R_C)$ is the energy associated with the Hall voltage drop across the cyclotron diameter; $E_H=J_xB/en_e$ is the Hall field and $R_C=v_F/\omega_c$ is the electron cyclotron radius (v_F is the Fermi velocity). Another notable nonlinear effect observed in the region of separated Landau levels (LLs) and weak dc is a strong reduction in the longitudinal resistance.[22] The main experimental features of the HIRO oscillations in the region of overlapped LLs and the suppression of resistivity in the region of separated LL can be explained by models based on electron transitions driven by the combined effects of impurity scattering and the strong dc excitation,[22–24] as well as by models that consider the formation nonequilibrium distribution function induced by the dc electric field.[25]

More recently new experiments have discovered that the effects of a direct dc current on electron transport can be quite dramatic leading to zero-differential resistance states (ZDRS).[26,27] As compared with the HIRO conditions, the ZDRS are observed under dc bias at higher magnetic fields (0.5–1.0 T) and lower mobility's (70–85 $\mathrm{m}^2/\mathrm{V\,s}$). At low temperature and above a threshold bias current the differential resistance vanishes and the longitudinal dc voltage becomes constant. Positive values for the differential resistance are recovered at higher bias as the longitudinal dc voltage slope becomes positive. Bykov *et al.*[26] discussed their experimental results following an approach similar to that of Andreev *et al.*[18] In terms of the differential longitudinal resistivity ρ_{xx} the stability condition reads

$$\rho_{xx}=\frac{\partial E_x}{\partial J_x}\geq 0. \tag{1}$$

The longitudinal differential resistance r_{xx} differs from ρ_{xx} by a geometrical factor $r_{xx}=\gamma\rho_{xx}$; where in the experiments γ is the ratio of the distance between the potential contacts to the width of the Hall bars. Hence, according to the condition in Eq. (1) the 2DES is unstable at negative-differential resistance $r_{xx}<0$. The presence of the ZDRS can be attributed to the formation of negative-differential resistance states (NDRS) that yields an instability that drives the system into a ZDRS. Similar results where obtained by Chen *et al.*[28]

In this paper we present a model to explain the formation of ZDRS. Both the effects of elastic impurity scattering as well as those related to inelastic processes play an important role. The model is based on the solution of the von Neumann

equation for 2D damped electrons, subjected to arbitrarily strong magnetic and dc electric fields, in addition to the weak effects of randomly distributed impurities. This procedure yields a Kubo-type formula for the electric density current that incorporates the nonlinear dependence on the electric field. Both inter- and intra-Landau-level transitions contribute to the density current, however as we are concerned with the separated LL range, the intra-Landau transitions play a dominant role. Considering a current controlled scheme, we obtain a set of nonlinear self-consistent relations that allow us to determine the longitudinal and Hall electric fields in terms of the imposed external current. Our model explicitly leads to a E_x-J_x nonlinear characteristic that predicts the existence of NDRS that in turn will evolve into the observed ZDRS. It is shown that the main experimental results[26] can be correctly reproduced if we assume a T^2 temperature dependence for the inelastic-scattering rate, consistent with electron-electron Coulomb interaction as the dominant inelastic process.

II. MODEL

We start with the Hamiltonian for an electron in the effective-mass approximation in two dimensions subject to a uniform perpendicular magnetic field $\boldsymbol{B}=(0,0,B)$, an in-plane electric field $\boldsymbol{E}=(E_x,E_y,0)$, and the impurity scattering potential $V(\boldsymbol{r})$. Hence the dynamics is governed by the total Hamiltonian $H=H_e+V$, with

$$H_e = H_0 + e\boldsymbol{E}\cdot\boldsymbol{x}, \tag{2}$$

here $H_0=\boldsymbol{\Pi}^2/2m$, m is the effective mass of the electron, e is the electron's charge, $\boldsymbol{\Pi}=\boldsymbol{p}+e\boldsymbol{A}$ is the velocity operator and the vector potential in the symmetric gauge is given as $\mathbf{A}=(-By,Bx)/2$. The impurity scattering potential is expressed in terms of its Fourier components

$$V(\boldsymbol{r}) = e^{-\eta|t|}\sum_i^{N_{im}} \int \frac{d^2q}{(2\pi)^2} V(q)\exp[i\boldsymbol{q}\cdot(\boldsymbol{r}-\boldsymbol{r}_i)], \tag{3}$$

where $\boldsymbol{r}_i$ is the position of the ith impurity and N_{im} is the number of impurities. The explicit form of $V(q)$ depends on the nature of the scatterers,[12] for simplicity we assume short-range uncorrelated delta scatterers characterized by a constant $V(q)$. A more detailed study should also cover charged scatterers.[12,24,29] The factor $\exp(-\eta|t|)$ takes care of the adiabatic switching of the impurity potential at the initial time $t_0\to-\infty$.

The motion of a planar electron in magnetic and electric fields can be decomposed into the guiding center operator coordinates $\boldsymbol{Q}$ and the relative coordinates $\boldsymbol{R}=(-\Pi_y,\Pi_x)/eB$, such that the position of the electron is given by $\boldsymbol{r}=\boldsymbol{Q}+\boldsymbol{R}$. The commutation relations for velocity and guiding center operators are $[R_x,R_y]=[Q_y,Q_x]=-il_B^2$, with all the other commutators being zero and $l_B^2=\hbar/eB$ is the magnetic length.

Our aim now is to compute the electric current density. In order to calculate the expectation value of the current density we need the time-dependent density matrix $\rho(t)$ which obeys the von Neumann's equation $i\hbar\partial\rho/\partial t=[H,\rho]$. We assume that in the absence of the impurity potential the density matrix reduces to the equilibrium density matrix given by $\rho_0=f(H_e)$, with $f(E)$ given by the Fermi distribution function. In order to solve the von Neumann's equation we apply three unitary transformations: the first two transformations exactly take into account the dynamics of the electric and magnetic fields, whereas the third transformation incorporates the impurity scattering effects to second order in time-dependent perturbation theory. First we consider the unitary transformation

$$\mathcal{W}(t) = \exp\left\{\frac{i}{\hbar}\left[\int \mathcal{L}dt + m\boldsymbol{v}\cdot\boldsymbol{R} + eB\boldsymbol{\xi}\cdot\boldsymbol{Q}\right]\right\}. \tag{4}$$

We recall that $\boldsymbol{R}$ and $\boldsymbol{Q}$ are operators. On the other hand $\boldsymbol{v}(t)$ is the "classical" electron velocity that evolves according to the equation of motion

$$\dot{\boldsymbol{v}} = -\frac{e}{m}\boldsymbol{E} - \omega_c\boldsymbol{v}\times\boldsymbol{e}_z - \frac{1}{\tau_{in}}\boldsymbol{v}, \tag{5}$$

here $\boldsymbol{e}_z$ is the unit vector normal to the plane of the system and the coordinate $\boldsymbol{\xi}(t)$ follows the drift of the electron's orbit, it is obtained from the solution of the equation

$$\dot{\boldsymbol{\xi}} = -\left(\frac{1}{B}\boldsymbol{E} - \frac{1}{\tau_{in}\omega_c}\boldsymbol{v}\right)\times\boldsymbol{e}_z. \tag{6}$$

Except for the damping terms, the equation of motion [Eq. (5)] follow from the variation in a classical Lagrangian[12] $\mathcal{L}=\frac{1}{2}m\boldsymbol{v}^2+e\boldsymbol{v}\cdot\boldsymbol{A}+e\boldsymbol{E}\cdot\boldsymbol{r}$. In order to incorporate dissipative effect we added the damping term $\boldsymbol{v}/\tau_{in}$ to the equations of motion. This procedure yields a simple scheme to incorporate dissipation to the quantum system. Recent magnetoresistance experiments[30,31] and theory[25] suggest that in 2DES, electron-electron interaction provide an important contribution to the inelastic-scattering rate, giving rise to $1/\tau_{in}\propto T^2$ temperature dependence, in our calculation we shall assume that the inelastic-scattering rate is dominated by the electron-electron interaction effect. By means of the transformation [Eq. (4)] the Hamiltonian H_e is diagonalized, the energy levels are given by the tilted LL,

$$\mathcal{E}_{\mu,k} = \hbar\omega_c\left(\mu+\frac{1}{2}\right) + \hbar\omega_k, \tag{7}$$

where $\omega_k=\boldsymbol{k}\cdot\boldsymbol{v}_d$, the drift velocity $\boldsymbol{v}_d$ is obtained from the solution of Eq. (5) and it is given as

$$\boldsymbol{v}_d = \frac{e\tau_i}{m}\frac{\boldsymbol{E}-\omega_c\tau_{in}\boldsymbol{e}_z\times\boldsymbol{E}}{1+\omega_c^2\tau_{in}^2}, \tag{8}$$

while $\boldsymbol{k}$ is a vector parallel to the direction of $\boldsymbol{v}_d$ and its magnitude is given by the eigenvalue of the guiding center operator projected along the direction of $\boldsymbol{v}_d$.

The transformation [Eq. (4)] renders the von Neumann equation into the following form

$$i\hbar\frac{\partial(\mathcal{W}\rho\mathcal{W}^\dagger)}{\partial t} = [H_0+V(t),\mathcal{W}\rho\mathcal{W}^\dagger].$$

The electric field term is conveniently removed from the Hamiltonian to produce a time-dependent impurity potential

$$V(t) = V\left[\boldsymbol{r} + \boldsymbol{\xi}(t) + \frac{1}{\omega_c}\boldsymbol{v}(t) \times \boldsymbol{e}_z\right]. \tag{9}$$

We now switch to the interaction picture through the unitary operator $\mathcal{U}_0 = \exp(iH_0 t/\hbar)$ and solve the remaining equation up to second order in time-dependent perturbation theory, obtaining yet another simplified version of von Neumann equation

$$i\hbar \frac{\partial}{\partial t}(\mathcal{U}\mathcal{U}_0 \mathcal{W}\rho\mathcal{W}^\dagger \mathcal{U}_0^\dagger \mathcal{U}^\dagger) = 0, \tag{10}$$

where the time evolution operator is given by

$$\mathcal{U} = 1 - \frac{i}{\hbar}\int_{t_0}^{t} V_I(s_1)ds_1 - \frac{1}{\hbar^2}\int_{t_0}^{t}\int_{t_0}^{s_1} V_I(s_1)V_I(s_2)ds_1 ds_2, \tag{11}$$

here $V_I(t) = \mathcal{U}_0 V(t)\mathcal{U}_0^\dagger$ is the impurity potential in the interaction picture. The formal solution to Eq. (10) is given by $\rho(t) = \mathcal{W}^\dagger \mathcal{U}_0^\dagger \mathcal{U}^\dagger \rho(t_0)\mathcal{U}\mathcal{U}_0\mathcal{W}$, where $\rho(t_0) = f(H_e)$ is the equilibrium density matrix at the initial time $t_0 \to -\infty$.

The current density is proportional to the thermal and time average of the velocity operator

$$\boldsymbol{J} = \frac{e}{S}\int_{-\infty}^{\infty} dt\ \mathrm{Tr}[\rho(t)\boldsymbol{\Pi}], \tag{12}$$

where S is the surface of the sample. By performing a cyclic permutation in the trace we obtain

$$\boldsymbol{J} = \frac{e}{S}\int_{-\infty}^{\infty} dt\ \mathrm{Tr}[\rho(t_0)\mathcal{U}\mathcal{U}_0\mathcal{W}\boldsymbol{\Pi}\mathcal{W}^\dagger \mathcal{U}_0^\dagger \mathcal{U}^\dagger]. \tag{13}$$

After a lengthy calculation an explicit expression for the current density is worked out, it splits into a Drude and an impurity-induced contribution,

$$\boldsymbol{J} = \boldsymbol{J}^D + \boldsymbol{J}^{im}. \tag{14}$$

The Drude contribution is given by $\boldsymbol{J}^D = n_e e \boldsymbol{v}_d$, where n_e is the electron density and the drift velocity is given in Eq. (8). The components of the impurity-induced density current can be expressed as

$$J_i^{im} = \frac{e\omega_c n_{im}}{\hbar^2}\sum_{\mu\mu'}\int \frac{d^2q}{2\pi}[f(\mathcal{E}_{\mu,q/2}) - f(\mathcal{E}_{\mu',-q/2})]G^i_{\mu\mu'}(q), \tag{15}$$

where $n_{im} = N_{im}/S$ is the impurity density; $i,j = x,y$; $\epsilon_{i,j}$ is the 2D antisymmetric tensor; and f is the Fermi distribution function evaluated at the tilted LL energies $\mathcal{E}_{\mu,q/2}$ and $\mathcal{E}_{\mu',-q/2}$ given by Eq. (7). The function $G^i_{\mu\mu'}$ is given by

$$G^i_{\mu\mu'} = |V(q)|^2 |D_{\mu\mu'}(z_q)|^2 \times \frac{q_i \Delta_{\mu\mu'} + 2|\epsilon_{ij}|q_j\omega_c\eta}{\Delta^2_{\mu\mu'} + 4\omega_c^2\eta^2}, \tag{16}$$

where

$$\Delta_{\mu\mu'} = [\omega_q + \omega_c(\mu - \mu')]^2 - \omega_c^2 + \eta^2 \tag{17}$$

and $\omega_q = \boldsymbol{q}\cdot\boldsymbol{v}_d$. Finally the matrix elements $D_{\mu,\nu}$ are given by

$$D_{\mu\mu'}(z_q) = \exp\left(-\frac{|z_q|^2}{2}\right) \times \begin{cases} z_q^{\mu-\mu'}\sqrt{\dfrac{\mu'!}{\mu!}}L_{\mu'}^{\mu-\mu'}(|z_q|^2), & \mu \geq \mu' \\ (-z_q^*)^{\mu'-\mu}\sqrt{\dfrac{\mu!}{\mu'!}}L_{\mu'}^{\mu'-\mu}(|z_q|^2), & \mu \leq \mu' \end{cases}, \tag{18}$$

where $z_q = l_B(q_x - iq_y)/\sqrt{2}$ and $L_\nu^{\mu-\nu}$ denotes the associated Laguerre polynomial.

According to the structure of Eqs. (14) and (15) the current density incorporates both a linear dependence on the electric fields in $\boldsymbol{J}^D$, as well as a nonlinear contribution through the argument dependence of $\boldsymbol{J}^{im}$ on ω_q. The term in Eq. (16) would present a singular behavior that is an artifact of the $\eta \to 0$ limit. This problem is solved by including the disorder broadening effects. A simple phenomenological prescription is dictated by retaining a finite value of η.[32] According to this prescription the density of states of the μ level would have the modified Lorentzian form given in Eq. (16). Furthermore, in order to take into account the known fact that the width of LLs depends on the magnetic field,[33] henceforth we shall consider $\eta = \Gamma\omega_c$.

The differential conductivity tensor is calculated from $\sigma_{ij} = \partial J_i/\partial E_j$. Finally the differential resistivity tensor is obtained from the inverse of the conductivity, that is, $\rho_{ij} = \sigma_{ij}^{-1}$.

In a current controlled scheme: the longitudinal density current is fixed to a constant value J_{dc} and there is no transverse current, J_y. This leads to a set of two implicit equations for the density current

$$J_x(E_x, E_y) = J_{\mathrm{dc}}, \quad J_y(E_x, Ey) = 0, \tag{19}$$

where the explicit expressions for the functions J_i are given in Eqs. (14)–(17). An approximated scheme to account for HIRO can be implemented if one fixes E_y to the value of the classical Hall field $E_y = E_H = BJ_{\mathrm{dc}}/en_e$ and considers $E_x \ll E_y$.[24] However the high nonlinearity present in ZDRS demands further improvement in the accuracy of the electric field components by a recursive application of Newton's method. To obtain the components of the electric field E_x and E_y, we start assigning guess values $E_x = E_{x_0}$ and $E_y = E_{y_0}$ that solve these relations in the absence of impurities (i.e., using only the Drude term). The first round of electric field computations are thus corrected by

$$\Delta E_x = \rho_{xx}J_x + \rho_{xy}J_y, \tag{20}$$

$$\Delta E_y = \rho_{yx}J_x + \rho_{yy}J_y. \tag{21}$$

The newly calculated values of the electric field are inserted in Eqs. (14) and (15) giving the corrected density current components. This process is carried out until the convergence criterion $|J_y/J_x| \sim 1 \times 10^{-15}$ is achieved.

Before we discuss the results for the ZDRS, we recall that the MIRO periodicity occurs in the regime of overlapping LL and can be explained by the Zenner tunneling between the tilted Landau levels.[19] At low temperature and assuming that $E_y \approx E_H$ we have $\omega_q \sim q_x J_x/en_e$, hence the resonant con-

dition in Eqs. (16) and (17) gives $\omega_q = q_x J_x / e n_e = l\omega_c$, where $l = \mu - \mu'$ is the index difference between the involved LL. This means that the impurity scattering transfers a momentum $q_x = k_x - k_x'$ to the electron causing a transition between the tilted LL. The dominant contribution is obtained at $q_x \approx \sqrt{8N_F}/l_B$, where we consider that the transition occurs in the vicinity of the Fermi level. Hence $N_F \approx E_F/\hbar\omega_c$ and the resonant condition is obtained as $J_x = e\omega_c\sqrt{n_e/8\pi l}$. However for the discussion or the ZDRS we are interested in the separated LL region that lies below the first HIRO peak and the dominant effect is provided by the intra-Landau transitions.

III. RESULTS AND DISCUSSION

In order to make a realistic comparison with the experimental results we have to estimate the values of the parameters in the model, as well as the temperature dependence of the mobility. As reported by Bykov *et al.*[26] we consider an electron density $n_e = 8 \times 10^{15}$ m^{-2}, and mobility $\mu = 100$ m^2 V/s at $T = 2$ K. The mobility is related to the single-particle lifetime τ_q as $\mu = e/m\tau_q$, and we assume that both the impurity scattering rate $1/\tau_{im}$ and the inelastic rate $1/\tau_{in}$ contribute to τ_q,[30,31] utilizing the Matthiessen's rule, we write

$$\frac{1}{\tau_q} = \frac{1}{\tau_{im}} + \frac{1}{\tau_{in}}, \quad \frac{1}{\tau_{in}} = \lambda \frac{(k_B T)^2}{\hbar E_F}, \tag{22}$$

where E_F is the Fermi energy. The expression for $1/\tau_{in}$ assumes that the inelastic rate is dominated by the electron-electron scattering ($\tau_{in} \equiv \tau_{ee}$) and we use the well-known estimate for $1/\tau_{ee} = \lambda(k_B T)^2/\hbar E_F$.[30,31,34,35] The parameter λ has to be experimentally determined but it is a constant on the order of the unity; here we fixed at $\lambda = 1$. Taking into account the previous information, we obtain that at $T = 2$ K the inelastic rate $1/\tau_{in}$ can be neglected as compared with $1/\tau_q$. Consequently the impurity contribution dominates $\tau_q \sim \tau_{im}$. For the case of short-range scatterers τ_{im} is simply related to the impurity potential and density.[12] The potential is written as $V(q) = 2\pi\hbar^2\alpha/m$, then the relation reads $1/\tau_{im} = 4\pi^2\hbar\alpha^2 n_{im}/m$ and we estimate $\alpha^2 n_{im} \sim e/4\pi^2\hbar\mu \sim 4.5 \times 10^{11}$ m^{-2}. Finally the broadening parameter is selected as $\Gamma = 0.04$.

Figure 1 shows the differential resistivity $\rho_{xx} = \partial E_x/\partial J_x$ as a function of the longitudinal dc density current J_x for a magnetic field $B = 0.784$ T and various values of the temperature. As the value of the temperature is reduced the differential resistance decreases approaching zero. We observe that at low temperature ($T < 2$ K) and above a threshold bias current ($J_x > 0.4$ A/m) the differential resistivity becomes negative. Positive values for the differential resistance are recovered at higher bias or higher temperatures.

The electric field E_x is plotted as a function of the longitudinal current J_x in Fig. 2. In order to compare with the experimental results, it is important to notice that E_x differs from the longitudinal voltage V_{xx} by a geometrical factor, given by the distance between the potential contacts in the sample. In this plot we observe negative slope regions below $T = 2$ K and above the current threshold $J_x > 0.4$ A/m (see inset of Fig. 2), in agreement with the ρ_{xx} negative values

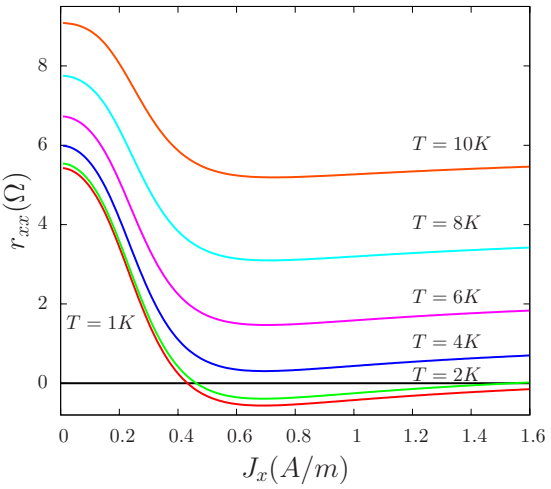

FIG. 1. (Color online) Differential resistivity ρ_{xx} as a function of the dc bias J_x for $B = 0.784$ T temperatures from $T = 1$ to 10 K.

observed in Fig. 1. According to Eq. (1) the stability condition is expressed as $\rho_{xx} \geq 0$.[26] Thus the regions in Figs. 1 and 2 that display a negative-differential resistivity are unstable and they must evolve into ZDRS to ensure stability. Accordingly, in the ρ_{xx}-J_x plots we must replace the NDRS portions of the curve by ZDRS and in the V_{xx}-J_x curves the negative slope regions must be amended by an horizontal line. This replacement is reminiscent of the Maxwell construction.[36] At higher values of J_x the differential resistivity as well as the longitudinal voltage slope become positive (Fig. 1). The observed behavior is originated in the nonlinear dependence of the impurity assisted current on the electric fields that in turns produces a nonlinear voltage-current characteristics when $\boldsymbol{E}$ is determined as a function of J_x by means of the iterative procedure described above.

Figure 3 display a series of plots of E_x field as a function of the longitudinal density current J_x at $T = 2$ K for various fixed values of the magnetic field that correspond to Shubnikov–de Haas oscillations maxima. The thin lines in-

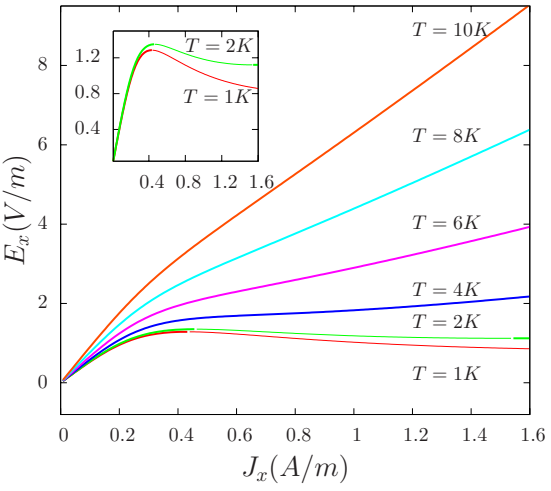

FIG. 2. (Color online) Electric field E_x as a function of the dc bias J_x for $B = 0.784$ T and for fixed temperatures ranging from $T = 1$ to 10 K.

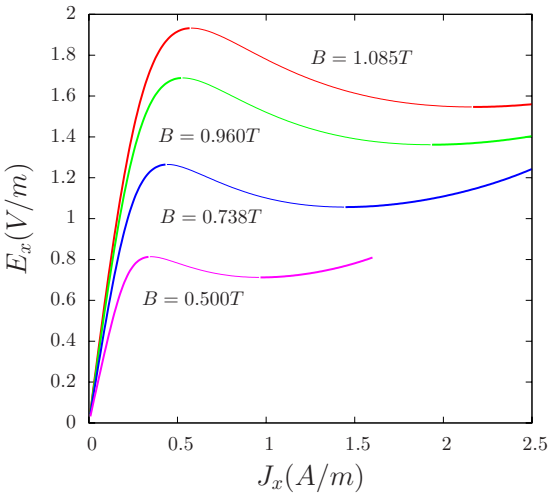

FIG. 3. (Color online) Electric field E_x as a function of the dc bias J_x for $T=2$ K and for fixed magnetic fields ranging from $B=0.5$ to 1.085 T. The thin lines indicate that $r_{xx}<0$.

dicate the formation of NDRS where the condition in Eq. (1) is violated and an instability that drives the system to a ZDRS is expected. As the magnetic field increases the width of the electric field plateaus and the value of threshold current required to produce NDRS increases.

The strong temperature dependence observed in these plots, consistent with the experiments, is originated from the interplay of the impurity and inelastic effects. In Fig. 4 we observe a plot of the calculated electric field E_x as a function of the temperature T. In this graph we also show experimental points extracted from Bykov *et al.*[26] [see Fig. 3(a)]. A qualitative good agreement is attained in the general trend of the E_x-T characteristics, although there is a difference in the absolute scale for the values of E_x; the difference is probably related to the precise determination of the distance between

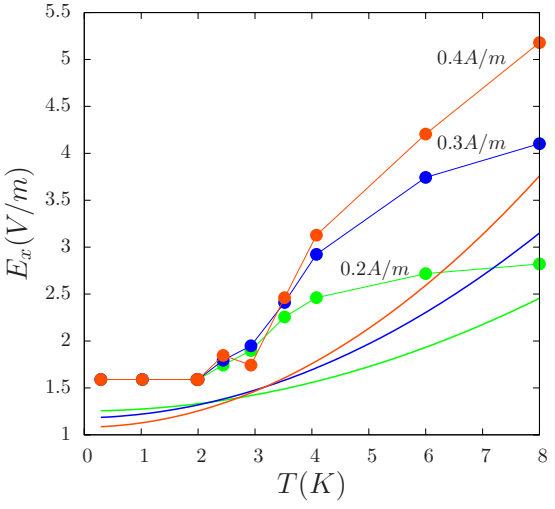

FIG. 4. (Color online) Electric field E_x as a function of the temperature T for three fixed values of the dc bias J_x and for a magnetic field $B=0.784$ T. The thick lines correspond to the theoretically calculated curves and the dots indicate the corresponding experimental values. The thin lines between the dots are for visual aid.

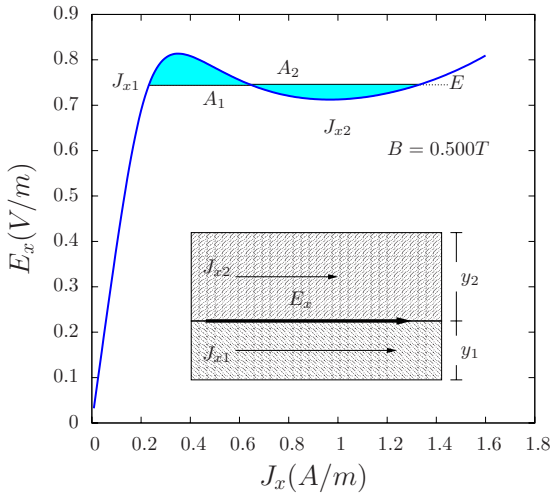

FIG. 5. (Color online) Electric field E_x as a function of the dc bias J_x for $T=2$ K and for magnetic field $B=0.5$ T. The negative differential resistivity line is replaced by the horizontal line, corresponding to a non uniform configuration with two values J_{x1} and J_{x2} for the density current with the same electric field E determined by the equal area rule $A_1=A_2$. The inset shows a possible domain wall configuration with two currents J_{x1} and J_{x2}.

the potential contacts. Both in the experimental and theoretical results we can clearly identify a crossing point for the curves at temperature $T_{th}\sim 3$ K. It signals the transition from the stable regime ($T>T_{th}$) to the unstable region ($T<T_{th}$) where the NDRS evolve into ZDRS. In the low-temperature regime ($T<T_{th}$) the impurity scattering dominates, whereas the temperature increases above T_{th} the inelastic scattering becomes important and the NDRS are no longer supported. Let us first assume that we can neglect the impurity scattering contribution, in the region $T>T_{th}$, the current density is then given by the Drude contribution; utilizing Eqs. (14)–(18) and the condition for the vanishing of the transverse current Eq. (19) yields

$$E_x \approx \frac{1}{\omega_c \tau_{in}} E_y \approx \frac{m}{e^2 n_e} \frac{J_x}{\tau_{in}} = \frac{1}{\pi \hbar^3} \left(\frac{m k_B T}{e n_e} \right)^2 J_x, \qquad (23)$$

where $E_y \approx E_H = B J_x / e n_e$ is approximated by the Hall electric field and the temperature dependence for τ_{in} in Eq. (22) is used. Both the $E_x \propto T^2$ dependence and the fact that E_x increases with J_x is observed in Fig. 4. On the other hand, in the region $T<T_{th}$, the dependence of E_x on J_x is inverted, an increase on the current reduces the value E_x leading to the generation of NDRS. In this case the results are dominated by the contribution of the intra-Landau transitions to the impurity-induced current Eq. (15).

The previous results show an excellent agreement with the experimental observations.[26] In order to throw further understanding of these phenomena it is convenient to analyze the structure of the voltage-current characteristics. Bykov *et al.*[26] proposed an *ad hoc* shape for the V_{xx}-I_{dc} dependence that suggest the formation of electric domains through the sample. Here we show that these conditions are predicted by our model. An isolated plot of the longitudinal electric field E_x as a function of the dc J_x is shown in Fig. 5.

In the region corresponding to the thin line the slope of the E_x-J_x plot is negative corresponding to a NDRS, however as previously discussed the system becomes unstable in this region. An approximate scheme (Maxwell construction) replaces the negative slope by a horizontal line, i.e., a ZDRS. The real reason for the appearance of a negative slope in the E_x-J_x plot is the implicit restraint of uniform electron density throughout the system. However in these regions configurations with a nonuniform current distribution turn out to be the equilibrium configuration of the system. The simplest possible pattern is a domain wall: two parts of the sample carry stable density currents J_{x1} and J_{x2} with the same value of E_x (see the inset of Fig. 5), the values are determined by the rule of equal areas ($A_1=A_2$). The Hall electric field E_H is discontinuous across the boundary leading to the accumulation electric charge. Due to the effect of E_x on the charge accumulation the boundary will propagate with a drift velocity $v_y=(\boldsymbol{E}_x^*\times\boldsymbol{B})/B^2$, leading to a current that oscillates in time. The accumulation of charge in the boundary of the domain wall and the current oscillations may be detectable experimentally. It should be observed that the situation is similar to the Gunn effect[37] that appears after an electric field in some materials reaches a threshold level, the mobility of electrons decrease as the electric field is increased, thereby producing negative resistance.

IV. CONCLUSIONS

In conclusion we presented a model to explain the formation of ZDRS. The model is based on the solution of the von Neumann equation for 2D damped electrons, subjected to arbitrarily strong magnetic and dc electric fields, in addition to the weak effects of randomly distributed impurities. This procedures yields a Kubo-type formula for the electric density current Eqs. (14)–(17) that incorporates the nonlinear dependence on the electric field. Considering a current controlled scheme, we obtain a set of nonlinear self-consistent relations that allow us to determine the longitudinal and Hall electric fields in terms of the imposed external current. The results show an excellent agreement with the experimental observations, at low temperature ($T<2$ K) and above a threshold bias current ($J_x>0.4$ A/m) the differential resistivity becomes negative. A correct comparison with the observed ZDRS is obtained by means of a "Maxwell-type construction." A fine balance between the impurity and inelastic-scattering rates is in play: at $T\leq 2$ K the inelastic rate is negligible and the impurity-induced current yields NDRS. However the rapid growth of $1/\tau_{in}\propto T^2$ leads to a transition to the stable region $T>3$ K. It is argued that the reason for the appearance of a negative slope in the E_x-J_x plot is the implicit restraint of uniform electron density throughout the system. However in these regions configurations with a nonuniform current distribution turn out to be the equilibrium configuration of the system. The simplest possible pattern is a domain wall. Although, NDRS may no be observable, it is important to identify the regions in which they are predicted because they are associated with physical effects that have been already observed, such as the ZDRS, and also to other effects that may be probably observed in future experiments: e.g., domain walls, current oscillations, etc.

ACKNOWLEDGMENTS

A. Kunold is receiving financial support from "Estancias sabáticas al extranjero" CONACyT and "Acuerdo 02/06" Rectoría UAM-A, and he wishes to thank INSA-Toulouse for their hospitality. We acknowledge support from UNAM Project No. IN118610.

*akb@correo.azc.uam.mx; kunold@insa-toulouse.fr
†torres@fisica.unam.mx

[1] M. A. Zudov, R. R. Du, J. A. Simmons, and J. L. Reno, Phys. Rev. B **64**, 201311(R) (2001).
[2] M. A. Zudov, R. R. Du, L. N. Pfeiffer, and K. W. West, Phys. Rev. Lett. **90**, 046807 (2003).
[3] R. G. Mani, J. H. Smet, K. von Klitzing, V. Narayanamurti, W. B. Johnson, and V. Umansky, Nature (London) **420**, 646 (2002).
[4] P. D. Ye, L. W. Engel, D. C. Tsui, J. A. Simmons, J. R. Wendt, G. A. Vawter, and J. L. Reno, Appl. Phys. Lett. **79**, 2193 (2001).
[5] V. I. Ryzhii, Sov. Phys. Solid State **11**, 2078 (1970).
[6] V. Ryzhii and V. Vyurkov, Phys. Rev. B **68**, 165406 (2003).
[7] J. Shi and X. C. Xie, Phys. Rev. Lett. **91**, 086801 (2003).
[8] S. I. Dorozhkin, JETP Lett. **77**, 577 (2003).
[9] A. C. Durst, S. Sachdev, N. Read, and S. M. Girvin, Phys. Rev. Lett. **91**, 086803 (2003).
[10] X. L. Lei and S. Y. Liu, Phys. Rev. Lett. **91**, 226805 (2003).
[11] M. G. Vavilov and I. L. Aleiner, Phys. Rev. B **69**, 035303 (2004).
[12] M. Torres and A. Kunold, Phys. Rev. B **71**, 115313 (2005).
[13] J. Iñarrea and G. Platero, Phys. Rev. B **76**, 073311 (2007).
[14] I. A. Dmitriev, A. D. Mirlin, and D. G. Polyakov, Phys. Rev. Lett. **91**, 226802 (2003).
[15] I. A. Dmitriev, M. G. Vavilov, I. L. Aleiner, A. D. Mirlin, and D. G. Polyakov, Phys. Rev. B **71**, 115316 (2005).
[16] I. A. Dmitriev, A. D. Mirlin, and D. G. Polyakov, Phys. Rev. B **70**, 165305 (2004).
[17] J. P. Robinson, M. P. Kennett, N. R. Cooper, and V. I. Fal'ko, Phys. Rev. Lett. **93**, 036804 (2004).
[18] A. V. Andreev, I. L. Aleiner, and A. J. Millis, Phys. Rev. Lett. **91**, 056803 (2003).
[19] C. L. Yang, J. Zhang, R. R. Du, J. A. Simmons, and J. L. Reno, Phys. Rev. Lett. **89**, 076801 (2002).
[20] A. A. Bykov, J. Q. Zhang, S. Vitkalov, A. K. Kalagin, and A. K. Bakarov, Phys. Rev. B **72**, 245307 (2005).
[21] J. Q. Zhang, S. Vitkalov, A. A. Bykov, A. K. Kalagin, and A. K. Bakarov, Phys. Rev. B **75**, 081305(R) (2007).
[22] W. Zhang, H.-S. Chiang, M. A. Zudov, L. N. Pfeiffer, and K. W. West, Phys. Rev. B **75**, 041304(R) (2007).
[23] X. L. Lei, Appl. Phys. Lett. **90**, 132119 (2007).
[24] A. Kunold and M. Torres, Physica B **403**, 3803 (2008).
[25] M. G. Vavilov, I. L. Aleiner, and L. I. Glazman, Phys. Rev. B **76**, 115331 (2007).
[26] A. A. Bykov, J. Q. Zhang, S. Vitkalov, A. K. Kalagin, and A. K.

Bakarov, Phys. Rev. Lett. **99**, 116801 (2007).
[27] N. Romero, S. McHugh, M. P. Sarachik, S. A. Vitkalov, and A. A. Bykov, Phys. Rev. B **78**, 153311 (2008).
[28] J. C. Chen, Y. Tsai, Y. Lin, T. Ueda, and S. Komiyama, Phys. Rev. B **79**, 075308 (2009).
[29] J. H. Davies, *The Physics of Low-Dimensional Semiconductors* (Cambridge University Press, Cambridge, 1998).
[30] A. T. Hatke, M. A. Zudov, L. N. Pfeiffer, and K. W. West, Phys. Rev. Lett. **102**, 066804 (2009).
[31] A. T. Hatke, M. A. Zudov, L. N. Pfeiffer, and K. W. West, Phys. Rev. B **79**, 161308(R) (2009).
[32] J. Sinova, T. Jungwirth, J. Kucera, and A. H. MacDonald, Phys. Rev. B **67**, 235203 (2003).
[33] T. Ando, A. B. Fowler, and F. Stern, Rev. Mod. Phys. **54**, 437 (1982).
[34] A. V. Chaplik, Sov. Phys. JETP **33**, 997 (1971).
[35] G. F. Giuliani and J. J. Quinn, Phys. Rev. B **26**, 4421 (1982).
[36] R. K. Pathria, *Statistical Mechanics* (Butterworth-Heinemann, Oxford, 1996).
[37] J. B. Gunn, Solid State Commun. **1**, 88 (1963).